Journal of ELECTRONIC MATERIALS, Vol. 41, No. 11, 2012
DOI: 10.1007/s11664-012-2237-9

Electrophoretic Deposition of Carbon Nanotubes on Silicon Substrates

ANIRBAN SARKAR[1,2] and DOOYOUNG HAH[1]

1.—Department of Electrical and Computer Engineering, Louisiana State University and A&M College, Baton Rouge, LA 70803, USA. 2.—e-mail: asarka4@lsu.edu

In recent years, the electrophoretic deposition (EPD) technique has been viewed as an attractive method for depositing carbon nanotube (CNT) thin films at room temperature, mostly on metal substrates. In this study, EPD has been performed to obtain deposits of CNTs on silicon substrates with various surface coatings. The process resulted in CNT film thicknesses up to ~15 μm on metal-coated silicon samples. The nanotubes exhibited preferential deposition and adhesion exclusively on the metal surfaces even when the direct-current (DC) voltage was supplied only to the silicon substrate, which was electrically isolated from the metal layer. The effects of electric field, deposition time, and underlying films on the thickness and surface roughness of the CNT film were studied. The adhesion strength of the CNT film was studied as well. The results obtained demonstrate the great potential of EPD of CNT thin films for a wide range of applications.

Key words: Carbon nanotubes, electrophoretic deposition, acid reflux

INTRODUCTION

Since the discovery of carbon nanotubes (CNTs) by Iijima,[1] substantial research has been pursued and reported regarding their physical and chemical properties. CNTs can be envisioned as sheets of graphene rolled into a cylindrical shape. The typical diameter and length of these nanotubes are 5 nm to 50 nm and 10 μm to 100 μm, respectively. Over the last decade of nanoscience research, most attention has been paid to optimization of nanotube synthesis by direct growth techniques such as arc discharge, laser ablation, and chemical vapor deposition (CVD). Nanotube growth conditions have been studied extensively, such as temperature, time, feedstock hydrocarbon precursors, nanometallic growth catalysts, and purification methods. Characterization of nanotubes after postsynthesis processing has been investigated comprehensively as well.[2,3] An emerging field of nanomaterials research is focused on device integration of CNTs on various substrates, exploring numerous applications such as metal– and polymer–CNT composites, field-emission devices, transparent electrodes for display systems, supercapacitors, electrochemical sensors, thin-film transistors, microelectromechanical systems (MEMS) devices, energy storage, plastic electronics, etc.[4–7]

Direct growth techniques for CNTs have achieved significant success in precise control of nanotube deposition. However, these approaches have a few drawbacks in process integration for some applications. The high growth temperature (typically ~900°C) and presence of unwanted residual catalyst and soot-like carbonaceous agglomerates in the final product restrict the incorporation of such CNTs into a wide range of technologies such as MEMS and plastic electronics. The need for an expensive high-vacuum system is another shortcoming. To mitigate these challenges, numerous room-temperature, low-cost, solution-based CNT thin-film coating methods have been developed.[8]

CNTs are hydrophobic and chemically inert in their pristine condition, which results in frequent agglomeration and subsequent precipitation in the solution during the dispersion and deposition steps. Various surface modification techniques are, therefore, employed to improve their stability and prevent deterioration of the suspension medium.[9,10]

(Received October 19, 2011; accepted May 24, 2012;

This process, also known as functionalization of the CNTs, can be achieved through either covalent or noncovalent reactions on the nanotube surfaces. Charged chemical moieties are introduced on the nanotube surface by this process. The electrostatic repulsive force between these moieties restricts significant agglomeration and entanglement of the dispersed nanotubes, leading to remarkable stability and extended lifetime of the suspension medium.

Using such dispersed CNTs in a suitable suspension medium, numerous innovative solution-based CNT coating techniques have been introduced, such as the "logs-on-a-river" approach, also known as the Langmuir–Blodgett (LB) method,[11] self-assembly of functionalized CNTs on chemically modified substrates,[12–14] linker-free, directed assembly of CNTs using self-assembled monolayer (SAM) molecules,[15] local surface charging,[16] dip coating,[17] drop casting,[18] spray coating,[19] spin coating,[20] inkjet printing,[21] Mayer rod coating,[22] etc.

One of the promising solution-based CNT coating techniques is electrophoretic deposition (EPD).[23–25] It is a low-cost, reproducible, room-temperature deposition approach, traditionally employed in the processing of ceramics, coatings, inks, and composite materials from colloidal solutions. EPD can be described by two essential processes. In the first step, charged particles dispersed in a solvent or an aqueous medium are stimulated to migrate towards the desired electrode by the application of a DC electric field across the suspension (electrophoresis). In the second step, the particles collect and adhere to the electrode surface and form a coherent deposit. Several theories have been proposed to explain the deposition and adhesion of particles on the desired substrates. Those are: (1) decrease in the interparticle repulsion and collapse of the particles to form a deposit due to increase in electrolyte concentration, (2) neutralization of the particles upon contact with the deposition electrode or the deposit, and (3) decrease in the repulsion between the incoming particles and between the deposit and the incoming particles due to thinning of the double layer.[23]

Among crucial application fields of EPD of CNTs are microelectronics and MEMS, where silicon substrates are used predominantly. However, research on EPD of CNTs has been, so far, concentrated mostly on metal substrates such as stainless steel,[24] aluminum, nickel, titanium, and glass plates with conductive coatings. Reports on EPD of CNTs on silicon substrates have been relatively few, thus offering an interesting research paradigm to investigate. In addition, to the best knowledge of the authors, an attempt to deposit CNT thin films on patterned metals atop insulating layers such as silicon dioxide and silicon nitride has been seldom made, even though these materials are commonly used in silicon technology.

It is worth mentioning another relevant method, i.e., dielectrophoresis (DEP), in conjunction with EPD. DEP has been investigated in deposition of CNTs on various substrates including silicon wafers. It relies on the motion of polarizable objects in response to an inhomogeneous alternating-current (AC) electric field.[26,27] Directed assembly and alignment of CNTs have been reported across patterned metal electrodes using DEP. The main motivation of this work, however, is to deposit CNTs as a thin film on silicon substrates, rather than directed assembly or alignment of a bundle of CNTs across metal electrodes. Therefore, EPD is more appropriate for this purpose.

The relevant sections of this study reveal pertinent details in regards to preparation of a CNT suspension for the intended EPD process and characterization of the deposited films, including their thickness, average surface roughness, electrical conductivity, and adhesion strength in relation to various deposition parameters.

EXPERIMENTAL PROCEDURES

The experimental procedure is divided into three sections: (a) preparation of a stable CNT solution for EPD, (b) substrate preparation, and (c) the EPD process.

Preparation of a CNT Solution

One hundred milligrams of as-obtained multiwalled CNTs [purity: $>95\%$; average wall thickness: 3 to 19 graphene layers; dimensions: 7 nm to 15 nm (O.D.) $\times$ 0.5 μm to 200 μm (length); CVD, Sigma-Aldrich, USA] were refluxed in 40 mL concentrated sulfuric (H_2SO_4) and nitric (HNO_3) acid (3:1 volume ratio). The solution was heated at 120°C for 45 min on a hot plate. The acid–heat treatment of the CNT solution resulted in a black slurry that was subsequently cooled for 1 h. The acid-refluxed tubes were then mixed with deionized (DI) water, and the solution was washed and filtered in medium retentive filter papers (pore size: $\sim$11 μm) repeatedly until the resulting solution indicated pH 7 (neutral). The solution was then placed inside a bath ultrasonicator for 2 h to obtain a stable CNT solution. The concentration of the CNTs in the final solution was slightly less than 1 mg/mL. The dispersed CNT solution as shown in Fig. 1a was kept inside a chemical hood undisturbed for 72 h to examine the stability of the solution. The CNT suspension did not indicate any visual signs of agglomeration, thus indicating stability for further processing.

Substrate Preparation

Silicon wafers (resistivity: 0 Ω cm to 100 Ω cm) were used in all the EPD experiments. Three different types of test samples were fabricated as described in Table I, using standard silicon processing techniques. For samples B and C, 280-nm-thick silicon dioxide was grown by thermal oxidation at 900°C, patterned by an ultraviolet (UV) photolithographic process, and wet etched by 48% HF solution to expose

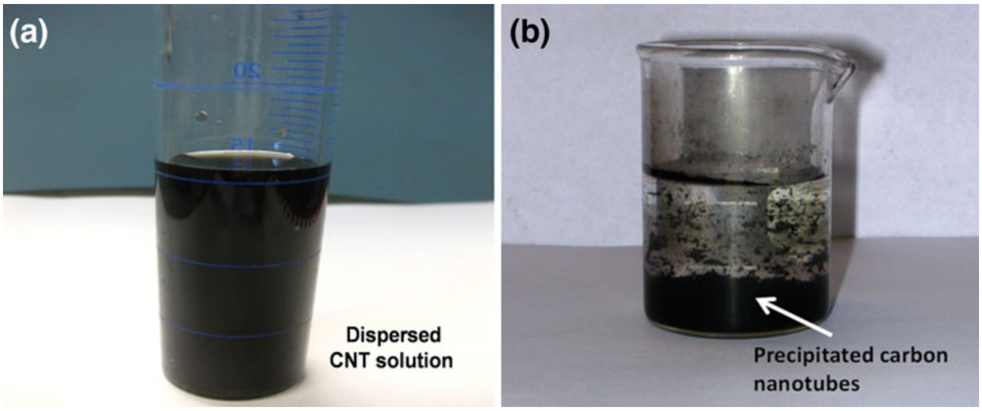

Fig. 1. (a) Dispersed CNT solution obtained after bath sonication of acid-refluxed CNTs, used for EPD experiments. (b) Degraded CNT solution with precipitated carbon nanotubes after a failed EPD attempt with bare silicon substrates (color online).

Table I. Layer structures of different types of samples used in the EPD experiments

Sample	Layer Structure
A	Al (300 nm)/Si
B	Al (300 nm)/SiO_2 (280 nm)/Si
C	Al (300 nm)/Si_3N_4 (150 nm)/SiO_2 (280 nm)/Si

the silicon layer underneath. For sample C, silicon nitride film of thickness 150 nm was deposited by low-pressure chemical vapor deposition (LPCVD; Nano Fabrication Center, University of Minnesota, USA), patterned by a photolithographic process, and etched by CF_4 reactive-ion etch (RIE) to expose the silicon dioxide underneath. A thin film of aluminum (300 nm) was finally deposited on all the samples by thermal evaporation and patterned by the lift-off technique.

EPD Process

EPD of CNTs was carried out in a purpose-built setup, as illustrated in Fig. 2, using a silicon sample as the anode and stainless steel (1.5 cm × 1 cm × 0.2 cm) as the cathode, which was degreased with acetone before use. The distance between the electrodes was fixed at 2 cm. Electrical connection to the anode was provided to the exposed silicon surface in all the EPD experiments. To investigate the effect of electric field and deposition time on the film thickness and quality, two sets of EPD conditions were tried: (i) varying voltage from 5 V to 30 V (or electric field from 2.5 V/cm to 15 V/cm) for constant deposition time of 3 min, and (ii) varying deposition time ranging from 0.5 min to 3 min for constant voltage of 30 V (or electric field of 15 V/cm). It should be noted that most of the voltage is applied across the EPD solution due to its high resistance (a few hundred kΩ). Before each set of experiment, the CNT solution was bath-sonicated for about 25 min to minimize bundled CNTs in the deposition process. After the deposition process, the samples were air-dried for 24 h.

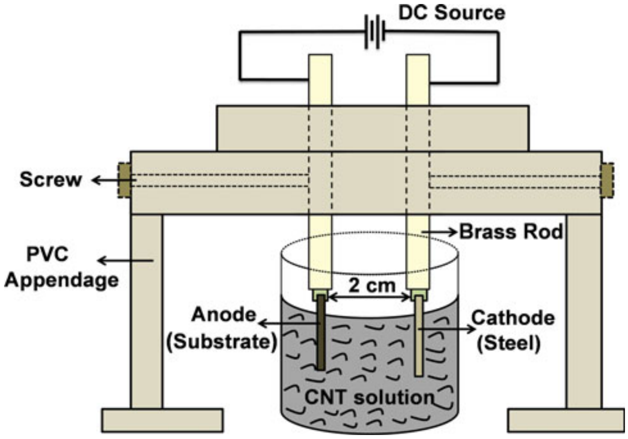

Fig. 2. Schematic diagram of an electrophoretic deposition setup (color online).

RESULTS AND DISCUSSION

Dispersion of the CNT solution

The acid–heat treatment of the as-purchased CNTs attaches negative carboxylic groups (–COOH) onto the surface of the tubes, thereby imparting negative surface charges. The resultant electrostatic repulsion prevents intertubular agglomeration and ensures appreciable stability of the CNT suspension during the dispersion process. Additionally, such aggressive treatment of the nanotubes aids in dismantling CNT agglomerates and dissolves residual metal catalysts, leading to simultaneous purification and shortening of the tubes.

As reported by Van der Biest and Vandeperre,[23] the desired approach in preparing an ideal suspension for EPD is to impart high zeta potential to the particles while maintaining low ionic conductivity of

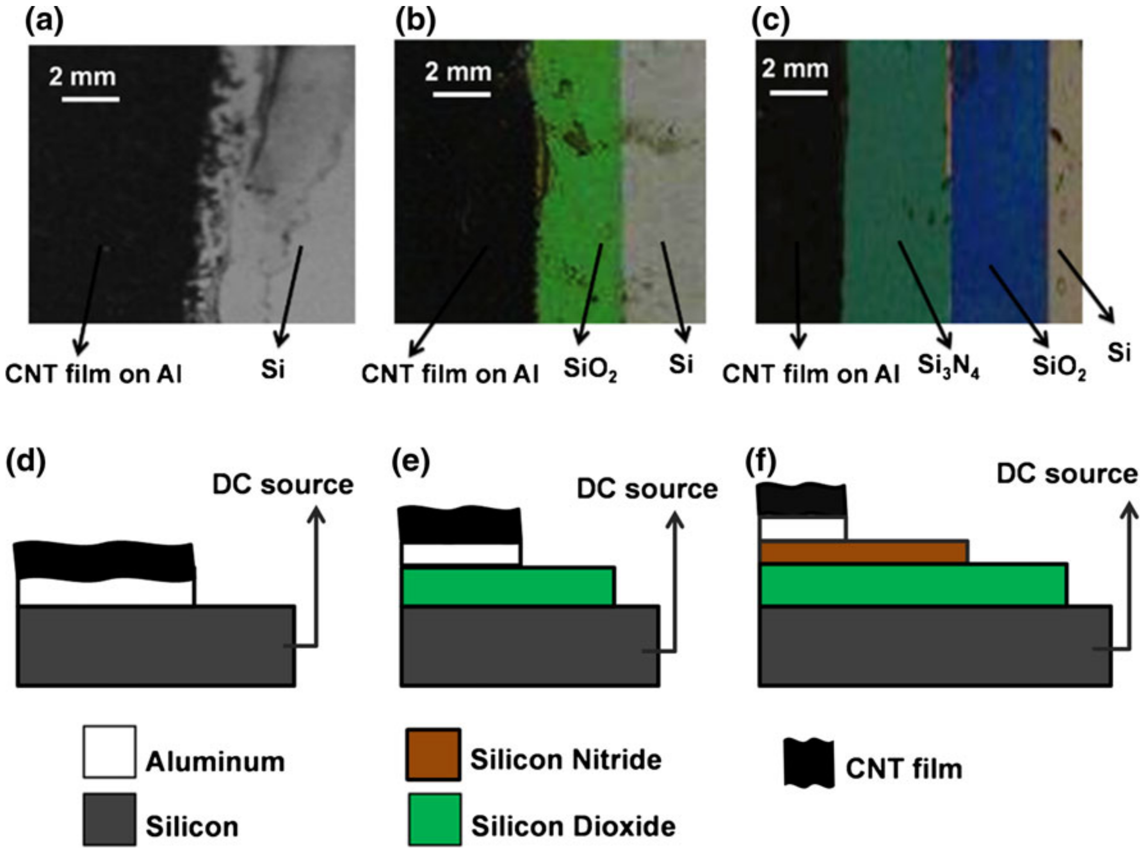

Fig. 3. Optical images (top view) of CNT film deposited on patterned aluminum on bare silicon or insulator (SiO$_2$ or Si$_3$N$_4$) at electric field of 10 V/cm for 3 min: (a) sample A, (b) sample B, and (c) sample C. Schematic cross-sectional diagrams of (d) sample A, (e) sample B, and (f) sample C (color online).

the suspension. The acid treatment of the pristine CNTs contributes enough negative charges on the surface of the nanotubes, resulting in sufficient negative zeta potential in neutral pH solution. The subsequent filtering and washing of CNT-COO$^-$ in DI water results in reduction of the ionic conductivity of the solution. These two processing steps assist in the preparation of a stable CNT-dispersed solution for electrophoretic coating after ultrasonic agitation.

Characterization of the Deposited CNT Film

Negative zeta potential of the acid-refluxed CNTs in the suspension[28] was substantiated by deposition of a CNT film at the anode surface of the EPD cell. One of the interesting results in all the EPD experiments was the selective deposition and strong adhesion of CNT film only on the aluminum surfaces, irrespective of the film underneath the aluminum layer. Figure 3a–c exhibits EPD results (deposition time: 3 min, electric field: 10 V/cm) on samples A, B, and C, respectively. Corresponding schematic cross-sectional diagrams of the samples are shown in Fig. 3d–f. As demonstrated by the figure, no deposition was observed on the exposed silicon, silicon dioxide, or silicon nitride surfaces, whereas profuse deposition was noticed on the aluminum surfaces in all the samples. Another noteworthy observation was the deposition of a CNT film on the aluminum surface even though the metal surface was not directly connected to the DC source in all the EPD tests. As mentioned earlier, the connection to the anode was imparted only on the exposed silicon surface for all the samples. It can be, thus, concluded that the silicon substrates acted as efficient anodes for all the EPD experiments to exert sufficient electrophoretic mobility to the acid-treated CNTs in the suspension. Under such an electrical connection scheme, it is also understood that the metal and the dielectric surfaces are charged positively as the silicon substrate during the EPD process, which is proved by continuous deposition of the CNTs on the metal surfaces.

Preferential adhesion of the CNT film on the metal surfaces can be partly attributed to hydrophilic interaction between the CNT (rendered hydrophilic during the acid oxidation step) and the aluminum surface. A similar explanation was provided by Oh et al.,[31] who performed liquid-phase fabrication of CNT cathodes. In our experiments, the effect of hydrophilic interaction was further demonstrated by insufficient coating and extremely poor adhesion of the CNTs on bare silicon substrates after EPD processes with a range of different durations and electric fields. After the samples were dried, only specks of scattered CNT aggregates were observed on the silicon surfaces. There exists another well-accepted theory, which explains the mechanism of EPD: formation of metal hydroxides on the target surface, which bind the CNTs with the substrate. However, this theory is based on the role of charger salts, which were not used in our experiments, and therefore cannot be applied to elucidate our results.

The role of metal as a preferred deposition surface was further investigated with EPD experiments on bare silicon substrates which were treated extensively with piranha solution (H_2SO_4:H_2O_2 = 1:1) as well as on native-oxide-etched silicon substrates. Piranha treatment significantly oxidizes the silicon surface, making it hydrophilic. EPD experiments with various conditions of electric field and deposition time resulted in very poor deposition of CNTs on the piranha-treated silicon surfaces. Multiple EPD attempts on the native-oxide-etched substrates resulted in very poor CNT deposition as well.

To verify the role of the interelectrode electric field in the EPD process, a silicon sample coated with aluminum was simply immersed in the CNT suspension for 3 min. After the immersion, only a loose, flimsy CNT layer was observed to adhere to the aluminum surface on the sample. The sample, after drying, left a minute amount of carbonaceous residues on the surface. Thus, it can be inferred from this experiment that hydrophilic interaction alone is not sufficient to enable CNT film deposition. The electric field in the EPD process needs to impart sufficient electrophoretic mobility to the nanotubes to overcome intertubular repulsion, to migrate, and to adhere onto the conducting surfaces. Therefore, formation of a CNT deposit on the conducting surfaces can be attributed to both the electrophoretic mobility of the charged CNTs in the suspension and adequate hydrophilic interaction on the target surface.

In a separate set of experiments, appreciable deposition of CNT films was also observed on copper surfaces on silicon substrates under similar EPD conditions and electrical connections. This result also substantiates the above explanation in regards to efficient CNT film deposition.

Microscopic Imaging and Raman Spectroscopy

Microstructural imaging of the deposited films was performed using an FEI Quanta 3D FEG dual-beam scanning electron microscope (SEM)/focused ion beam (FIB) at acceleration voltage of 20 kV to 30 kV. The samples were imaged as produced. Figure 4 shows scanning electron microscopy images of the CNT film deposited on aluminum-coated

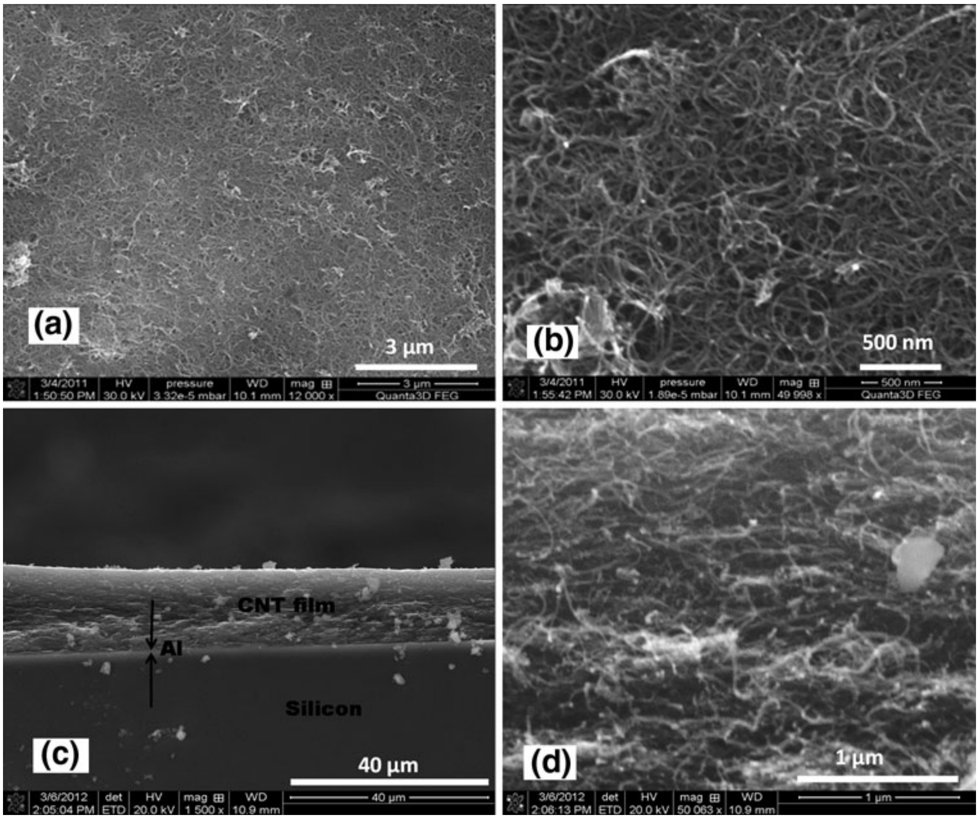

Fig. 4. Scanning electron microscopy images of deposited CNT film on sample A. (a) (Top view) CNT film showing appreciable packing density without voids, (b) (top view) magnified image of the CNT film, (c) (cross-section) view of the deposited CNT film and (d) (cross-section) magnified image of the CNT film.

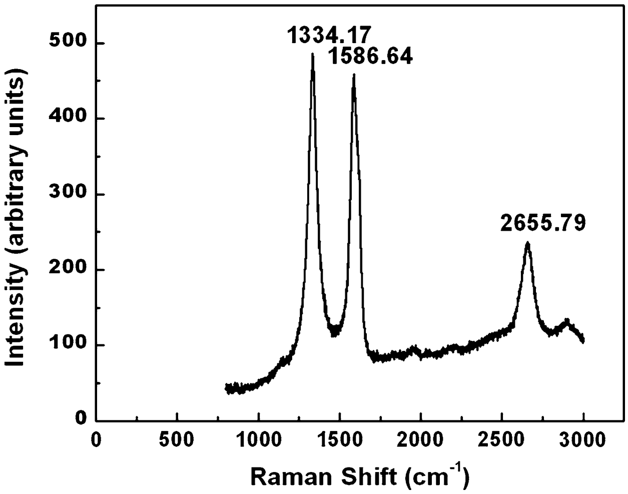

Fig. 5. Raman spectrum of carbon nanotube film deposited on sample A by 2 min of EPD at applied electric field of 10 V/cm.

silicon substrates. The images indicate appreciable homogeneity and packing density without any microscopic voids in the film. They also show the random nature of the CNT deposition, i.e., without any regular alignment.

The deposited CNT film was further characterized with Raman spectroscopy. Figure 5 shows the Raman spectra of the CNT film deposited on sample A for 2 min at applied electric field of 10 V/cm. The peak for the disorder-induced D-band was seen to occur at ~1330 cm^{-1}, and those for the tangential G-bands occurred at ~1580 cm^{-1} and ~2700 cm^{-1} for samples A, B, and C. Absence of the prominent radial breathing modes in the Raman spectra was noted for all scans. The Raman spectroscopy results, thus, conclusively indicate the presence of multiwalled nanotubes in the deposited CNT films.

Electrical Resistivity

Resistivity measurement of the deposited CNT films was performed by the four-point probe measurement technique. A dense film of CNT was obtained after 3 min of deposition at 15 V/cm on indium tin oxide (ITO)-coated glass substrates. The resistivity of the CNT film was measured to be ~7 × 10^{-5} Ω cm, while that of the ITO coating was ~3 × 10^{-4} Ω cm.

Adhesion Strength

Both qualitative and quantitative tests were performed to evaluate the adhesion strength of the CNT films deposited on the aluminum surface. The qualitative tests include: (a) the Scotch tape test in accordance with the American Society for Testing and Materials (ASTM) D-3359-97 standard,[32] and (b) ultrasonication test. A procedure known as the direct pull-off (DPO) method was used as the quantitative test.[33]

Qualitative Tests

(a) *Scotch tape test* This test method is widely used to establish whether the adhesion of a coating to a substrate is at a generally acceptable level. Test method A, one of the standard methods in ASTM D-3359, was applied to 10 different samples. The method involves making an X-cut in the film, application of a pressure-sensitive tape over the cut, and 180° rapid peeling of the tape. The adhesion is assessed qualitatively on a scale from 0 to 5, with 5 as the best adhesion result (no peeling or removal) and 0 as the worst (removal beyond the area of the X). The adhesion of the CNT film was rated close to 4 since only trace peeling of the film was noted. The results indicate appreciable adhesion quality of the CNT films.

(b) *Ultrasonication test* CNT-film-coated samples were immersed in deionized water and kept inside an ultrasonicator cleaning system (frequency: 55 kHz, output power: 200 W) for 10 h to 12 h. After the long period of ultrasonication, no noticeable detachment of the CNT film from the aluminum layer was observed.

Quantitative Test: Direct Pull-Off (DPO) Method In this method, a tensile force of increasing magnitude is applied on the specimen until the film is detached from the substrate. More precisely, the procedure involves:

(a) Attachment of the substrate to a table by means of a strong adhesive such as epoxy,
(b) Attachment of a pulling device (e.g., a brass bar) onto the target film by means of an adhesive (e.g., epoxy or cement), and
(c) Pulling of the bar in the direction perpendicular to the film, noting the force at film detachment.In addition, the broken specimens were visually examined to validate the location or origin of the breakage. Five samples underwent the DPO test. In all cases, the fractures occurred either at the aluminum–silicon interface or in the middle of the aluminum film, at 0.5 MPa to 1 MPa. This value is comparable to the adhesion strength of aluminum films deposited on soda lime glasses, as reported by Mittal.[30] These tensile test results indicate that the adhesion strength between the CNT film and the aluminum surface is greater than 0.5 MPa to 1 MPa. To obtain more accurate values for the CNT film adhesion strength, it is necessary to use a better (i.e., stronger and with higher adhesion strength) metal film for the CNT deposition.

Thickness and Surface Roughness

The overall yield and homogeneity of the CNT films are influenced by the concentration of the dispersed CNT suspension[29,30] and the EPD parameters such

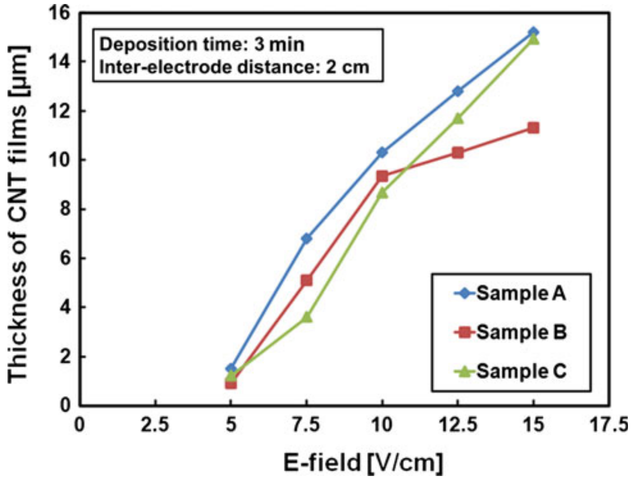

Fig. 6. Thickness of CNT films on samples A, B, and C as a function of applied electric field at constant deposition time of 3 min (color online).

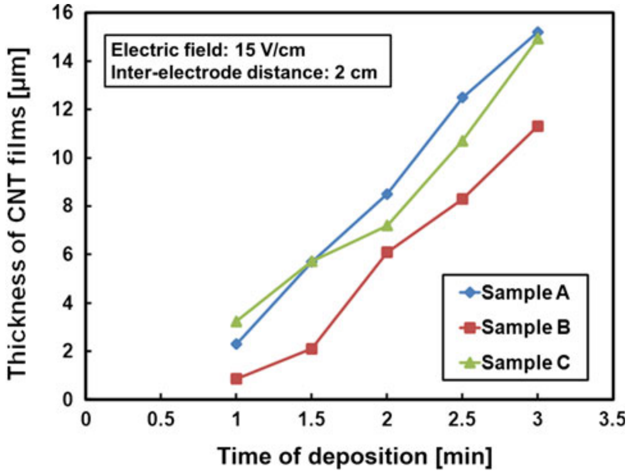

Fig. 7. Thickness of CNT films on samples A, B, and C as a function of deposition time at constant applied electric field of 15 V/cm (color online).

as the interelectrode electric field and deposition time. Optical examination of the deposited films on samples A, B, and C in the experiments indicated varying coating quality depending on the EPD conditions. For more quantitative analysis, film thickness and average surface roughness measurements were performed using a KLA-Tencor P-II surface profiler. For the surface roughness measurement, surface profile scanning was performed for 10 times for each sample, and the average value was calculated.

It was observed that, for constant deposition time of 3 min, the thickness of the CNT film deposited on the aluminum-coated samples showed an increasing trend with increasing interelectrode electric field, as shown in Fig. 6. Film thicknesses as high as ~15 μm on samples A and C and ~11 μm on sample B were observed for the highest electric field, i.e., 15 V/cm. It has also been observed that, at low electric field (< 5 V/cm), there exists a "no-coating" zone where the deposition is almost negligible or results in low-quality, nonuniform coating without appreciable adhesion to the substrates. Figure 6 also shows the appearance of a kink and relatively lower film thickness at high electric field for sample B. The reason for such a kink and lower CNT film thickness cannot be determined at this time and is under further investigation.

The thickness of the CNT film deposited on the aluminum-coated samples displays an increasing nature with increasing deposition time (Fig. 7) under constant electric field of 15 V/cm. The "no-coating" zone is also observed at fairly low deposition time (< 1 min). The deposited film thickness on sample B is somewhat lower than those on samples A and C over the entire range. This agrees with the results presented in Fig. 6, which shows thinner film deposition in the case of sample B at high electric field.

The EPD results, thus, indicate that longer deposition time and higher electric field result in the deposition of a thicker CNT layer. This observation is in accordance with the deposition characteristics reported by Thomas et al.,[29] who performed CNT film deposition by EPD on stainless-steel substrates.

Surface roughness measurements of the CNT film coating under varying deposition time (1 min to 3 min) and electric field (5 V/cm to 15 V/cm) indicated the effects of both parameters on film quality. Figure 8 shows the surface roughness measurements of the CNT films for varying electric field. The surface roughness values are excessively high (~300 nm to 350 nm) for deposition at low electric field (5 V/cm). This can be attributed to uneven initiation of the deposition around the "no-coating" zone. Surface roughness also tends to increase at high electric field (≥10 V/cm). This observation agrees with the report by Thomas et al.,[29] who pointed out that CNTs may aggregate under high electric field. Figure 9 exhibits the surface roughness measurement results of the CNT films for varying deposition time. The roughness profile exhibits a similar trend to that seen in Fig. 8: high surface roughness for short and long deposition time.

Post-EPD Agglomeration of the CNT Solution

One of the interesting observations throughout the EPD experiments was the agglomeration and subsequent sedimentation of the CNTs, resulting in an inhomogeneous solution after failed EPD attempts. The solution showed clusters of CNT flakes floating in the solution during the EPD process, which eventually precipitated as CNT agglomerate at the bottom. Figure 1b shows the degraded CNT solution after a failed EPD attempt on a bare (i.e., without any dielectric or metal coating) silicon sample, which was repetitively observed in the case

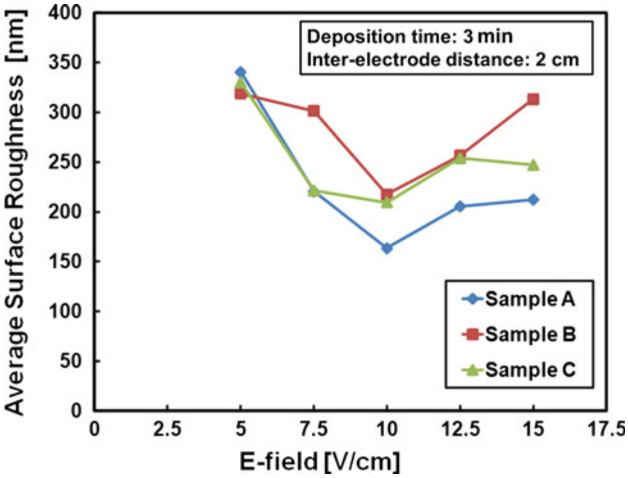

Fig. 8. Average surface roughness of CNT films deposited on samples A, B, and C as a function of applied electric field at constant deposition time of 3 min (color online).

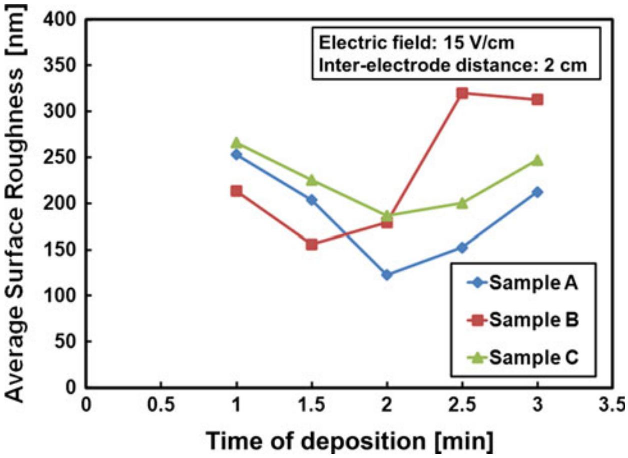

Fig. 9. Average surface roughness of CNT films deposited on samples A, B, and C as a function of deposition time at constant applied electric field of 15 V/cm (color online).

of bare silicon samples regardless of the EPD conditions. This phenomenon can be explained by the possible interaction between the CNTs which failed to adhere to the silicon surfaces and the incoming surge of functionalized nanotubes from the solution migrating towards the anode. Such interaction may lead to adhesion of CNTs to one another to form clusters during the EPD process, and thus eventually, result in agglomeration in the postdeposition period. In contrast to the solution behavior with bare silicon substrates, the CNT solution after successful EPD experiments on metal-coated silicon substrates showed remarkable stability and reusability for substantial deposition attempts.

CONCLUSIONS

EPD of CNTs has been successfully performed from acid-refluxed stable CNT-dispersed suspension on metal-patterned silicon substrates with or without insulating layers (SiO_2 and Si_3N_4) in between. The CNT films exhibited selective deposition and excellent adhesion on aluminum surfaces, irrespective of the insulator layers underneath and electrical connection to the anode surface. The quality of the deposited film, i.e., thickness and surface roughness of the CNT coatings, was observed to be dependent on the EPD process parameters, i.e., applied electric field and deposition time. CNT film as thick as 15 μm was achieved on silicon substrates at applied electric field of 15 V/cm for 3 min. Microscopic imaging and Raman spectroscopy confirmed deposition of multiwalled nanotubes. Deposited CNT film showed reasonably good adhesion strength and electrical conductivity. These results confirm that the solution-based, low-cost, room-temperature EPD approach for nanotube film deposition can lead to a wide range of potential applications including silicon-based electronics and MEMS technologies.

ACKNOWLEDGEMENTS

The research was supported, in part, by the Louisiana Experimental Program to Stimulate Competitive Research (EPSCoR, LEQSF(2011)-PFUND-233), funded by the National Science Foundation and the Board of Regents Support Fund.

REFERENCES

1. S. Iijima, *Nature* 354, 56 (1991).
2. M.S. Dresselhaus, *Carbon* 33, 871 (1995).
3. M. Meyyappan, *Carbon Nanotubes: Science and Applications*, 1st ed. (Boca Raton: CRC, 2004).
4. R.H. Baughman, A.A. Zakhidov, and W.A. de Heer, *Science* 297, 787 (2002).
5. M. Terrones, *Annu. Rev. Mater. Res.* 33, 419 (2003).
6. J. Wang, *Electroanalysis* 17, 7 (2005).
7. G. Gruner, *J. Mater. Chem.* 16, 3533 (2006).
8. L. Hu, D.S. Hecht, and G. Gruner, *Chem. Rev.* 110, 5790 (2010).
9. R. Rastogi, R. Kaushal, S.K. Tripathi, A.L. Sharma, I. Kaur, and L.M. Bharadwaj, *J. Colloid Interface Sci.* 328, 421 (2008).
10. J. Lee, M. Kim, C.K. Hong, and S.E. Shim, *Meas. Sci. Technol.* 18, 3707 (2007).
11. P. Yang, *Nature* 425, 243 (2003).
12. Y. Wang, D. Maspoch, S. Zou, G.C. Schatz, R.E. Smalley, and C.A. Mirkin, *Proc. Natl. Acad. Sci. USA* 103, 2026 (2006).
13. J. Liu, M.J. Casavant, M. Cox, D.A. Walters, P. Boul, W. Lu, A.J. Rimberg, K.A. Smith, D.T. Colbert, and R.E. Smalley, *Chem. Phys. Lett.* 303, 125 (1999).
14. S.G. Rao, L. Huang, W. Setyawan, and S. Hong, *Nature* 425, 36 (2003).
15. M. Lee, J. Im, B.Y. Lee, S. Myung, J. Kang, L. Huang, Y.-K. Kwon, and S. Hong, *Nat. Nanotechnol.* 1, 66 (2006).
16. L. Seemann, A. Stemmer, and N. Naujoks, *Nano Lett.* 7, 3007 (2007).
17. M.D. Lay, J.P. Novak, and E.S. Snow, *Nano Lett.* 4, 603 (2004).
18. J.A. Bardecker, A. Afzali, G.S. Tulevski, T. Graham, J.B. Hannon, and A.K.-Y. Jen, *J. Am. Chem. Soc.* 130, 7226 (2008).
19. J.H. Kim, K.-W. Nam, S.B. Ma, and K.B. Kim, *Carbon* 44, 1963 (2006).

20. M.C. LeMieux, M. Roberts, S. Barman, Y.W. Jin, J.M. Kim, and Z. Bao, *Science* 321, 101 (2008).
21. J.-W. Song, J. Kim, Y.-H. Yoon, B.-S. Choi, J.-H. Kim, and C.-S. Han, *Nanotechnology* 19, 095702 (2008).
22. B. Dan, G.C. Irvin, and M. Pasquali, *ACS Nano* 3, 835 (2009).
23. O.O. Van der Biest and L.J. Vandeperre, *Annu. Rev. Mater. Sci.* 29, 327 (1999).
24. A.R. Boccaccini, J. Cho, J.A. Roether, B.J.C. Thomas, E. Jane Minay, and M.S.P. Shaffer, *Carbon* 44, 3149 (2006).
25. M.P. Ryan, A.R. Boccaccini, and I. Corni, *J. Eur. Ceram. Soc.* 28, 1353 (2008).
26. P. Li and W. Xue, *Nanoscale Res. Lett.* 5, 1072 (2010).
27. B.R. Burg and D. Poulikakos, *J. Mater. Res.* 26, 1561 (2011).
28. K. Esumi, M. Ishigami, A. Nakajima, K. Sawada, and H. Honda, *Carbon* 34, 279 (1996).
29. B.J.C. Thomas, M.S.P. Shaffer, S. Freeman, M. Koopman, K.K. Chawla, A.R. Boccaccini, *Proceedings of the 2nd International Conference on Electrophoretic Deposition*, vol. 314 (Key Engineering Materials, 2006), pp. 141–146.
30. B.J.C. Thomas, A.R. Boccaccini, and M.S.P. Shaffer, *J. Am. Ceram. Soc.* 88, 980 (2005).
31. S.J. Oh, J. Zhang, Y. Cheng, H. Shimoda, and O. Zhou, *Appl. Phys. Lett.* 84, 3738 (2004).
32. ASTM D3359-02, *Standard Test Methods for Measuring Adhesion by Tape Test* (ASTM International, 2002).
33. K.L. Mittal, *Electrocompon. Sci. Technol.* 3, 21 (1976).